EUROPEAN FUSION DEVELOPMENT AGREEMENT

EFDA–JET–PR(03)39

R.J. Buttery, T.C. Hender, D.F. Howell, R.J. La Haye, S. Parris, O. Sauter,
C.G. Windsor and JET EFDA contributors

On the Form of NTM Onset Scalings

On the Form of NTM Onset Scalings

R.J. Buttery, T.C. Hender, D.F. Howell, R.J. La Haye[1], S. Parris[2], O. Sauter[3], C.G. Windsor and JET EFDA contributors*

[1]EURATOM/UKAEA Fusion Association, Culham Science Centre, Abingdon, OX14 3DB, UK
[2]General Atomics, San Diego, USA.
[3]Clare College, Cambridge, United Kingdom.
[4]Centre de Recherches en Physique des Plasmas, Association EURATOM-Confédération Suisse, EPFL, 1015 Lausanne, Switzerland.
** See annex of J. Pamela et al, "Overview of Recent JET Results and Future Perspectives", Fusion Energy 2000 (Proc. 18th Int. Conf. Sorrento, 2000), IAEA, Vienna (2001).*

Preprint of Paper to be submitted for publication in
Nuclear Fusion

EUROPEAN FUSION DEVELOPMENT AGREEMENT

EFDA–JET–PR(03)39

R.J. Buttery, T.C. Hender, D.F. Howell, R.J. La Haye, S. Parris, O. Sauter,
C.G. Windsor and JET EFDA contributors

On the Form of NTM Onset Scalings

On the Form of NTM Onset Scalings

R.J. Buttery, T.C. Hender, D.F. Howell, R.J. La Haye[1], S. Parris[2], O. Sauter[3], C.G. Windsor and JET EFDA contributors*

[1]EURATOM/UKAEA Fusion Association, Culham Science Centre, Abingdon, OX14 3DB, UK
[2]General Atomics, San Diego, USA.
[3]Clare College, Cambridge, United Kingdom.
[4]Centre de Recherches en Physique des Plasmas, Association EURATOM-Confédération Suisse, EPFL, 1015 Lausanne, Switzerland.
** See annex of J. Pamela et al, "Overview of Recent JET Results and Future Perspectives", Fusion Energy 2000 (Proc. 18th Int. Conf. Sorrento, 2000), IAEA, Vienna (2001).*

Preprint of Paper to be submitted for publication in
Nuclear Fusion

ABSTRACT.

Theoretically, the normalised plasma pressure (β) at which an NTM is triggered is expected to depend on normalised Larmor radius (ρ^*) and normalised collisionality (ν), and this has formed the basis for the way in which NTM onset scalings are quoted on many devices. However, new analyses of JET data shows that such ρ^* - ν based scalings are non-predictive, with discharges largely following such scalings over the majority of their duration while in H-mode. Neural network techniques indicate a key additional parameter to include is sawtooth period, providing a better degree of predictability. Indeed, this parameter appears more important than ρ^* in predicting NTM onset. Analysis using cases where sawteeth are modified by localised heating and current drive, indicates that it is the sawtooth which governs where it is *along* the NTM onset scaling trajectory that the NTM is triggered, rather than leading to departures from the scaling. Finally, exploring data from cross-device similarity experiments shows that the different devices, rather than lining up with one scaling, appear to be displaced in β - ρ^* space, with similar absolute values for the range in NTM onset β in each device. This suggests that a simple ρ^* based extrapolation for ITER may be inappropriate, and that NTM threshold levels may be more directly related to absolute value of β, suggesting a higher β threshold for ITER, at least if large sawteeth are avoided.

1. INTRODUCTION

Traditionally, Neoclassical Tearing Mode (NTM) threshold scalings are quoted in terms of a dependence of β (the ratio of plasma thermal energy to magnetic energy) on normalised ion Larmor radius (ρ^*) and normalised ion collisionality (ν) [1,2,3,4,5]. There is some variation in this according to the type of β used, and choices of global or local variables, poloidal or toroidal ρ^*, and normalisation for collision frequency. Nevertheless with most versions of these scalings in the various devices analysed, a near linear dependence of β on ρ^* is usually obtained, while collisionality scalings are fairly weak (with around zero exponent on JET, 0.23 on ASDEX Upgrade, and 0.43 on DIII-D) [1]. This appears to be well motivated by the underlying theory, and indeed such results are seen as an important validation of that theory, and the trends for ITER. However, analysis from JET presented in this paper shows that such approaches not only omit key physics ingredients, but can also be almost entirely non-predictive, even within one series of discharges where conditions were carefully maintained constant.

In this paper we re-examine the experimental evidence for $\beta \sim \rho^*$ NTM onset scalings, considering how they arise, and whether other physics effects are more important. We start in section 2 with a brief summary of the underlying theory and explain how this can lead to a $\beta \sim \rho^*$ type of scaling. We go on in section 3 to compare the resulting form against JET data, considering in particular how well NTM onset scalings (based on fitting β at NTM onset to ρ^* and ν dependencies) perform at predicting the time of mode onset in a particular series of controlled slow β ramp up experiments. Having found the scalings unsatisfactory (due to co-linearity between the NTM onset scaling and discharge evolution), in section 4 we employ neural network techniques to search for other controlling parameters. This finds that ρ^* and ν parameters are only of marginal benefit in predicting mode

onset, while sawtooth period is more important. In section 5 we go on to explore trends in a wider variety of discharges from JET, considering cases where the sawtooth period has been manipulated by localised current drive, and also comparing against discharge evolutions from cases used in JET entries to the ITER H mode data base. This highlights the key result for JET - that ρ^* - ν based NTM onset scalings actually describe the natural discharge evolution, which follows a remarkably well correlated and relatively narrow clustering in β - ρ^* space. The actual time of NTM onset appears to be governed by sawtooth period. We widen our exploration of NTM onset scalings in section 6, to compare the data across devices. Here we find similar ranges in β at NTM onset for each device (irrespective of size), with results displaced between the devices in β - ρ^* space. We discuss interpretation of these observations and possible theoretical explanations in section 7, before concluding in section 8.

We start the analysis using the local parameters most directly related to the expected NTM drive terms (poloidal β, β_p, and poloidal ρ^* both measured at the NTM resonant surface), although later in the paper we move to more noise resilient parameters of global β_N (defined as $\beta.aB_T/I_p$, with a being minor radius, I_p being plasma current and B_T being toroidal field) and toroidal ρ^*, which are less subject to details of profile and gradient terms, but otherwise exhibit similar trends.

2. FORMALISM– ORIGINS OF ρ^*, ν BASED SCALINGS

The choice of ρ^* and ν as the main governing scaling parameters is motivated by the underlying physics models for NTMs, which can be described by the modified Rutherford equation [6] for the time evolution of an island of size w:

$$\frac{\tau_r}{r_s^2}\frac{dw}{dt} = \Delta' + a_{bs}\,\varepsilon^{1/2}\,(L_q/L_p)\,\frac{\beta_p}{w}\left(\frac{1}{1+w_d^2/w^2} - \frac{w_{pol}^2}{w^2}\right) \qquad (1)$$

This is expressed in terms of the tearing stability parameter (Δ'), bootstrap current ($a_{bs}\beta_p/w$ term), ion polarisation effect (w_{pol} term) and additional transport effects in the island (w_d term). β_p is the ratio of plasma pressure to poloidal magnetic field pressure at the NTM resonant surface. L_q and L_p are scale lengths for safety factor and pressure gradients respectively, ε measures the ratio of the minor radius, r_s, of the resonant surface to its major radius, and τ_r is the resistive time scale. Usually either an ion polarisation current term (w_{pol}) [7] or finite island transport term (w_d) [8] is used to model the small island size stabilisation physics, although there are additional effects when w is close to the ion banana width [9]. Although there remain uncertainties in both of these models, each can lead to similar ρ^* and ν dependence of NTM thresholds. For example the ion polarisation current term can be characterised using [7],

$$w_{pol} \approx [\, g(\nu, \varepsilon)\,(L_q/L_p)\,\varepsilon\,]^{0.5}\,\rho_{i\theta} \qquad (2)$$

where 'g' is a function of normalised collisionality, $\nu = \nu_i/ew_e^*$, with g=1 for ν <<1, and g= $\varepsilon^{-3/2}$ for ν >>1; ν_i is the ion collision frequency, ω_e^* is the electron diamagnetic frequency, and ρ_{iq} is the

poloidal Larmor radius, all taken at the resonant surface. The constant of proportionality actually depends on the natural island propagation frequency in the zero radial electric field frame of reference [10] and is somewhat uncertain, both experimentally and theoretically. Nevertheless, folding this back into Eq. (1) and solving for marginal growth (dw/dt=0) at a given island size (w=w_{seed}), gives a form for the onset value of β_p:

$$\sqrt{\frac{L_q}{L_p}}\ \beta_{onset} = -r_s\,\Delta'.\rho^*_{i\theta}.\frac{w_{seed}/{w_{pol}}^2}{[1-(w_{pol}/w_{seed})^2]}\ .\ g\ (\nu,\varepsilon) \qquad (3)$$

is obtained, where $\rho_{i\theta}^{\ *} = \rho_{i\theta}/r_s$. A similar form can be obtained for the finite island transport model, as discussed in Refs [1] and [11], assuming a heat flux limited approach to allow for low collisionality [8]. We see that the small island size terms introduce the need for a finite 'seed' island size, w_{seed}, which must result from some other process, which we refer to as 'seeding'. Below this island size the stabilisation will become stronger and the island decay away, as confirmed experimentally [12]. Thus one might expect that the discharge follows some trajectory in (β, $\rho_{i\theta}^{\ *}$, ν) space (possibly with regular failed seeding events) before crossing the threshold dictated by Eq. (3) at which an NTM occurs. As we shall see later in the paper, this turns out not to be applicable, at least in terms of simple (β, $\rho_{i\theta}^{\ *}$, ν) parameters.

An important ingredient missing from the above formalism is the seeding process. This is not generally well understood experimentally at present [13], and as highlighted above, enters into the modified Rutherford equation in a non-linear way. The only attempt to date to fit data with a full physics model (ie one that includes all the relevant processes associated with onset of an NTM), was that of La Haye et al. [1]. This included terms for the seeding process due to sawteeth, obtaining a seed island size based on a model combining forms for sawtooth amplitude, mode coupling and dynamic shielding effects. In this model, the size of this seed island is then effectively compared with the threshold size required for neoclassical growth to evaluate the condition for NTM onset. This approach was valuable in testing physics models against existing data and highlighting the potential for a possible upturn in 3/2 NTM thresholds as ITER-relevant ρ^* levels were reached. However many aspects remain to be validated, while the overall approach needs to be better constrained if it is to have a predictive capability [14]. Nevertheless this approach did predict a threshold scaling in terms of ρ^* and ν for a given 'type' of sawtooth (in deuterium plasmas with only neutral beam heating), and achieved a reasonable match with data.

3. NEW ANALYSES OF JET DATA

New studies of discharges on JET show that the situation is somewhat more complex than a simple crossing of thresholds in β, ρ^*, ν parameter space. The initial problem with such approaches was identified with the observation that simple ρ^*, ν based fits to JET data, did not predict the time of the onset of the NTM. We start from the discharge series studied in Ref [13]. In this series neutral beam heating power was slowly ramped up until an NTM was triggered (usually by a sawtooth). All plasmas were of the same q_{95} and shape, with only slight variations in heating power ramp

rates, but also some discharge to discharge changes in toroidal field (with plasma current in proportion) and gas puff levels. It was observed that for very similar time-histories, some discharges had an onset of the NTM very much later, and at higher β, than others, despite very similar conditions and time histories for control parameters. To explore this effect we compared one of the† 'late-onset' NTM cases with the observed NTM onset threshold scalings for the discharge series. The onset appears to be fairly well described across the discharge series by a form in terms of local parameters at the q=3/2 surface:

$$(L_q/L_p)^{0.5}\beta_p = 16.2\ \rho_{i\theta}^{*\ 1.11\pm0.21}\nu^{-0.14\pm0.07} \qquad (4)$$

as illustrated in Fig 1. However applying this to the late onset case we find that this predicts that the NTM onset threshold is reached early on in the discharge, and stays close to the predicted threshold (which varies with time according to ρ^* and ν values) for some seconds before the NTM actually occurs, despite β_N rising by ~50%. This is shown in Fig.2, where the open circles indicate the ratio of $(L_q/L_p)^{0.5}\beta_p$ to the above fit form (rhs of Eq. 4), based on $\rho_{i\theta}^*$ and ν. This situation is not rectified by moving to more noise resilient parameters (global β_N «q$\rho_{i\phi}^*$, the local toroidal ρ_i^*): the solid squares in Fig.2 indicate the ratio of global β_N to fitted onset threshold based on toroidal Larmor radius (at the resonant surface) normalised to minor plasma radius (virtually no collisionality dependence is found in such fits):

$$\beta_N = 95.5\ \rho_{i\phi}^{*\ 0.71\pm0.14} \qquad (5)$$

This observation seems to suggest that scalings based on such parameterisations are a necessary, but not sufficient condition for NTM destabilisation on JET, and further physics must be involved.

A wider examination of this discharge series, as shown in Fig.3, indicates that in fact the main feature of the fit, Eq. (4), is to approximate the time evolution of the main heating phase as a whole, with individual discharges running close to co-linearity with the scaling. Indeed, the scatter of the discharges about the NTM onset fit is very similar to the scatter in the onset thresholds about this same fit, as shown in Fig 1. It should be noted that the clustering towards a single line in this parameter space appears to be a feature of the accessible operational space for these NTM discharges. As local $\beta \sim n.\rho^{*2}$ (n being density, with all quantities taken at the resonant surface), the approximately linear relation between β and ρ^* in Fig.3 indicates an inverse relation between density and ρ^* (perhaps indicating a 'natural' density that varies with heating power in these predominantly neutral beam fuelled plasmas).

Thus ρ^* and ν alone are not sufficient to describe the NTM onset requirement. This is somewhat surprising, given the attempts to standardise the seeding process in these experiments by using only NBI heating, with similar ramp-up waveforms and otherwise largely identical plasmas. The physics arguments leading to Eq. (3) suggest that ρ^* and ν should be the main parameters governing NTM

onset, while one might reasonably expect that additional physics variations, such as in the sawteeth that trigger the mode, depend on ρ^*, ν, or β, as in Ref [1].

4. APPLICATION OF NEURAL NETWORK TECHNIQUES TO THE JET DATA

In order to search for the controlling parameter for this process, and gain further insight into the physics governing the NTM onset, neural network techniques were employed. A wide range of up to 25 parameters (including dimensionless parameters such as β_N, ρ^*, ν, plasma internal inductance, q_{95}, and plasma shape, as well as a wide range of dimensional parameters such as toroidal field, neutral beam heating power, minor radius, sawtooth precursor amplitude, and sawtooth period) were fed into the network, which was then trained and optimised to predict the time of NTM onset. This was based on a wider database of 30 NTM and 5 non-NTM discharges, all using only neutral beam heating. Input data was taken at the time of each sawtooth crash leading up to the NTM onset. Testing of network performance was always performed on a 'leave one out' basis, with a given network type being trained on all discharges but the one used for testing, the process repeated for each discharge in turn to compile an overall performance statistic. This allowed an optimally trained network to be genuinely tested for predictability against the whole data set. Various network structures and equivalent-time parameters (eg time or β) were explored. The choice of input parameters for the network was automatically optimised, by exploring the effects of removal or addition of each input parameter from the initial list specified, each time retraining and re-testing the network, before choosing the best adjustment to make. This process was repeated until no further reduction in the test residual (ie. the sum of the squares of the differences between predicted time to NTM and actual time to NTM) could be obtained. A similar optimisation was made in the number of hidden units.

Results from the optimum network are shown in Fig.4 where predicted time to NTM is compared with actual time to NTM across the discharge series. The most important observation is that in nearly all cases, unlike the simple ρ^* based predictions, the network gets the correct trend, with predicted time to the NTM onset falling as the actual NTM onset is approached. This should be contrasted with Figs 2 and 3 where we see that for simple ρ^* - ν based scalings, β reaches the onset fit prediction early on and remains at this level for arbitrary time and rise in β. Surprisingly, it was found that the best performing network used just three input parameters: sawtooth period ($\tau_{sawtooth}$), β_N and $\rho_{i\phi}^*$. Introducing further parameters decreased network performance (effectively confusing the network with non-useful data). It is also interesting that given both measurements of sawtooth period and average magnetic amplitude of the sawtooth precursor, the network optimisation found sawtooth period to be far more significant. This is somewhat puzzling as one might expect that an amplitude measurement of the sawtooth would relate more directly to the driving of a seed island (we discuss this further in the next section). Also, as seen in Fig.4, the network actually identified two types of discharge, with predictability for the lower clump more limited (but still yielding the correct trend). This lower clump of discharges corresponds to cases where the NTM onset is later, at higher β, when plasma parameters are less rapidly changing.

The relative importance of the three best physics parameter was studied by exploring the variation in the test residual with one or two parameters removed. To provide a more intuitive measure of success, shots were also counted as successful (ie not 'errors') if they passed between the grey regions in Fig 4 - thus successful shots must have an NTM onset predicted to be imminent close to the actual time of NTM onset, but not give a strong onset probability ('false positive') too early. The results are shown in Table 1. Of greatest interest is the observation that sawtooth period appears even more important than $\rho_{i\phi}^{*}$ in governing NTM onset. The removal of $\rho_{i\phi}^{*}$ leads to imperceptible rises in errors and residuals (compare lines 1 and 2 or lines 3 and 4 of Table 1). However, the use of the sawtooth period offers improvements in predictability when it is combined with β_N as a network input. As expected for a bootstrap driven mode β_N remains the most important parameter, and performs reasonably well on its own, in terms of the test residual value (but crucially loses resolution close to NTM onset, so higher errors). Use of $\rho_{i\phi}^{*}$ on its own performed better than sawtooth period on its own, as this parameter has a closer correlation with β_N, thus it can act as an indication of the β_N value. Interestingly the addition of ν as a network parameter gives no improvement in performance. This is consistent with the very weak collisionality dependence observed in JET NTM onset scalings.

The neural network results show that it is important to include the sawtooth seeding process in NTM scaling to have a predictive capability. The role of the sawtooth is not very surprising in the context of theoretical developments [6,7,8,9,15] showing how seed island size is expected to affect NTM thresholds, and more recent results from JET using Ion Cyclotron Resonant Heating (ICRH) [16] to raise NTM thresholds by reducing sawtooth periods. Although variation of sawtooth behaviour in NBI discharges has been observed previously [17], the degree to which it enters into the NTM onset scalings even in these NBI only discharges is surprising, particularly that its significance is greater than that of $\rho_{i\phi}^{*}$.

5. THE ROLE OF SAWTEETH AND COMPARISON WITH WIDER DATA-SETS FROM JET

To explore the role of sawteeth in more detail, it is interesting to compare trajectories of NBI only cases with those using ±90° phasing ion cyclotron current drive in the vicinity of q=1 to stabilise/ destabilise the sawteeth. These are plotted in Fig.5(a) in terms of β_N versus $\rho_{i\phi}^{*}$ using the more noise resilient quantities global β_N and local toroidal $\rho_{i\phi}$ from now on, in order to reduce random error (although more physically motivated local parameters lead to similar conclusions). Some scatter in NTM threshold levels with ICRH is expected as this will also depend on ICRH power level and precise deposition location. There is also some difference in trajectories at low $\rho_{i\phi}^{*}$, associated with differences in plasma profiles when -90^{o} ICRH is a large fraction of the total heating power. Nevertheless, even though the range of the data has been considerably extended, the NTM onsets (symbols) are still largely co-linear with the discharge trajectories (lines). The different categories of discharge (±90∞ RF and NBI only) largely appear to line up. Thus rather than allowing a departure from the expected NTM onset scaling, the sawteeth merely govern how far along the trajectory the

plasma progresses before an NTM commences - as was also observed for the beam only cases. Thus +90∞ RF cases, where the RF stabilises the sawteeth, leading to less frequent but much larger events, have relatively low β_N onset values, while -90^o cases (with small frequent sawteeth) occur at higher β_N and later in the discharge.

The role of sawtooth period can be observed directly in the data shown in Fig 6, where we see that the ICRH can often lead to much longer sawteeth and lower NTM β thresholds. From this figure we also see that long sawtooth periods can be obtained in NBI-only discharges (usually the first sawtooth following transition to H mode after a large step up in heating power)†– this also results in low NTM β thresholds. Note that it is also possible to access high β without 3/2 NTMs but with long sawtooth periods in some cases on JET. The relevance of the sawtooth period parameter, as opposed to some other sawtooth amplitude measurement, is somewhat puzzling. From theoretically based arguments about how the NTM is seeded (for example from mechanisms such as forced reconnection and toroidal coupling [15]), one might expect that a measure of the sawtooth amplitude to be more appropriate, for example: soft X ray crash size, or magnetic precursor amplitude. Nevertheless, the empirical observation from JET (and also the result of the neural network analysis) is that the sizes of these other quantities are much less well correlated with NTM onset β levels. Conversely sawtooth period clearly plays a strong role, with low β NTM thresholds almost always associated with long sawteeth. It is possible that some of the models discussed in section 7 may relate more to the sawtooth period quantity (perhaps because longer periods allow more time for the pressure profile to evolve), though this is clearly an issue that needs further study, alongside resolving the physics of the NTM seeding process.

We note that the dependence of β_N on $\rho_{i\phi}^*$ at the NTM onset is somewhat steeper in Fig.5(a) than that expected from the fit to NBI only data (Eq.5) - a fit to the whole data set in Fig.5(a) for NTM onset yields a dependence $\beta_N \sim \rho_{i\phi}^{*1.5}$. This reflects the larger parameter range providing better constraints on the fit. (It also largely explains previously observed increases of NTM thresholds compared to onset scalings when sawteeth were modified using -90^o phasing ICRF [18]). It is worth noting that even with the modified form ($\beta_N \sim \rho_{i\phi}^{*1.5}$) for the onset scaling, the conclusions from Fig.2 remain unchanged, with many discharges exceeding the 'threshold' requirement at an early stage, well ahead of NTM onset. Thus these results still highlight the importance of using additional control parameters in the NTM onset scalings.

The clustering of NTM discharges about a trend-line in Fig.5(a) has been explored further by comparing the NTM cases with more non-NTM data taken from JET entries in the ITPA global H mode confinement database [19]. These include a wide range of NBI and ICRF heated plasmas, including cases with higher plasma current and toroidal field than the NTM discharges. Cuts have been made on the data to limit it to similar shape (triangularity between 0.2 and 0.33, elongation between 1.5 and 1.65) and q_{95} (between 3.1 and 3.6) as the NTM discharges. The ITPA data is plotted in red in Fig.5(b), with the NTM discharges from Fig.5(a) now all in black (NTM onset points marked by blue circles). The broader range of parameters involved in the ITPA database plasmas somewhat breaks the near-monotonic relationship between β_N and $\rho_{i\phi}^*$. Nevertheless, a

surprisingly strong correlation still emerges, largely consistent with the NTM discharges. This indicates that to a large degree NTM onset scalings of the form $\beta \sim \rho^*$ might arise from general operational and confinement properties of ELMy H mode discharges, rather than the underlying NTM physics.

6. CROSS MACHINE STUDIES

The above arguments indicate that present NTM onset scalings for NBI heated discharges merely represent the typical discharge trajectories for the configuration of plasma used. So what governs the NTM onset and how can the thresholds be extrapolated to ITER? As an example of trends, the La Haye cross-device paper [1] corrected out collisionality dependence using (different) power law fits for each device (note this gives zero collisionality exponent for JET) to explore the ρ^* dependence (where the ρ^* form used is the local $\rho_{i\phi}{}^*$ at the resonant surface throughout this section). Correcting in this manner to ν =0.08 raises some of the β thresholds from the smaller devices to make an approximate line in β - ρ^* space for JET, DIII-D and ASDEX Upgrade (although the degree of alignment depends on choice of ν value extrapolated to). Performing a full fit using the physics model of Ref [1], one can infer various possible scalings that extrapolate this downwards towards ITER-relevant low ρ^* values, with possible upturns at low ρ^* [14].

However, noting that the JET collisionality range largely overlaps that of DIII-D and ASDEX Upgrade, an alternative approach is to just plot the raw data at NTM onset as β_N versus ρ^*, as shown in Fig.7(a). In this case we see that, somewhat remarkably, all of the devices have similar ranges for the β_N at NTM onset, merely displaced in ρ^* value. There is no general trend towards lower β_N thresholds, or a lower maximum value for mode onset, as we go up in device size! Even if the expected collisionality dependence from the full model of Ref [1] is used to correct for this variation, the situation is not changed. This is shown in Fig.7(b), where we have scaled the β_N value of each point according to:

$$\beta_N \text{ (Fig.7(b))} = \beta_N \text{\_exp} \times Fit(\rho_{i\phi}{}^* \text{\_exp}, \nu \text{\_ave}) \,/\, Fit(\rho_{i\phi}{}^* \text{\_exp}, \nu \text{\_exp})$$

where: "_exp" refers to experimental value, "_ave" refers to average value over the data set, and,

$$Fit\,(\rho^*_{i\theta}.\ \nu) = \frac{0.057 \times 5.95\ \rho_{i\phi}^{*3\alpha}\, \nu^{\alpha}}{\dfrac{1}{1 + 0.62^2\ \rho_{i\phi}^{*2/3-6\alpha}\ \nu^{-2\alpha}} - \dfrac{(1+56.5\nu)/(1+3.1\nu)}{5.95^2\ \rho_{i\phi}^{*6\alpha} \nu^{2\alpha}}}$$

as taken from Ref [1] with $\rho_{i\phi}{}^*$ in units of 10^{-3} and $\alpha = 0.46$. Whilst this collisionality correction makes the ASDEX Upgrade and DIII-D data (which occupy fairly separate ranges in collisionality) produce a somewhat more consistent trend, the larger size JET device remains displaced in β - ρ^* space, with a similar range in β_N at NTM onset to the smaller devices.

7. DISCUSSION

With similar levels for NTM onset - β_N, despite different size devices, a key question must be

whether ITER might expect to see similar thresholds in terms of absolute β_N values, rather than the low thresholds inferred from $\beta \sim \rho^*$ based scalings? There is some physics justification for such a possible conclusion. Careful analysis of the 3/2 NTM onset on JET shows that magnetic coupling based models [1,15] (which are of a type that might lead to a linear β - ρ^* scaling on present devices) do not appear to explain the majority of NTM seeding events on JET [13]; there are large frequency mismatches between 2/2 and 3/2 harmonics, and there is generally little correlation with a 3 wave match criterion (between 4/3, 1/1 and 3/2 mode frequencies). In contrast there are other physics models for NTM seeding, which can lead to a behaviour more related to absolute value of β_N, as we discuss below:

Theoretical work has indicated the possibility of proximitw to ideal pressure driven kink limits leading to poles in Δ' [20] for 2/1 tearing modes, thereby triggering 2/1 NTMs. The principles involved can be generalised to other mode numbers and ideal instabilities. Indeed, further theoretical work has recently shown how this might apply to a particular high β sawtooth triggered 3/2 NTM onset case in DIII-D [21]. This may not be the only possible explanation of NTM seeding. For example changes in plasma rotation associated with the sawtooth event could change the size and sign of ion polarisation effects [10], thus driving formation of a seed island. With any of these approaches, the underlying tearing mode stability could vary rapidly as the appropriate criteria (such as the ideal stability limit) is approached, thereby explaining the lack of decaying seeds prior to NTM onset in many cases on JET [13]. It therefore remains a key task of NTM studies to help test and resolve this seeding mechanism for more cases.

CONCLUSIONS

NTM theory suggests a linear dependence of the NTM onset threshold in β, normalised Larmor radius, and a weak (but variable) positive dependence on normalised collisionality. Consequently these parameters are often used as the basis for quoting the NTM onset threshold scaling. Indeed the fact that the data appears to conform to such a scaling is often taken as a validation of NTM physics and a key property of their scaling behaviour. However, we have observed that these formulations appear to be entirely non-predictive on JET, both in terms of local and global parameters. Instead the scalings largely describe the time evolving trajectories of the discharges, arising from the natural confinement properties of the plasma. Even when wider data sets are considered (including cases with ICRH modified sawteeth, or pulses used for confinement scaling databases), NTM onset points largely lie on top of the usually followed discharge trajectory in β - ρ^* space. Thus generally there appears to be little evidence for a clear 'threshold' in β on JET. Further, comparing data from across devices shows that NTM onset events occupy similar ranges in β_N, rather than scaling with device size, and do not align to a single $\beta_N(\rho^*, \nu)$ scaling.

Neural network analysis confirms the significant role of the sawtooth period, even in NBI-only heated discharges, leading to a network that is at least capable of predicting the right trends. They also find the ρ^* and ν parameters to be only marginally useful in predicting NTM onset, while the

sawtooth period is much more helpful. Exploring a wider JET discharge set, which includes sawtooth control experiments, shows more generally how the sawtooth acts as a key controlling factor as to where along the discharge evolution (and onset scaling) it is that the NTM is triggered. These also confirm the sawtooth period as the key controlling parameter.

These considerations suggest a simple ρ^* based extrapolation to ITER may be inappropriate, and point to the possibility of an NTM seeding process more directly related to the absolute value of β_N. Thus it is possible that the NTM onset threshold on ITER may be higher than expected from a simple extrapolation with ρ^*. We have speculated on how such trends might arise from alternate seeding mechanisms, although clearly further work is required to resolve the seeding issue and explain the role of sawtooth period. Despite these encouraging trends,†we must also not ignore the substantial progress and apparent validation of physics models, which clearly indicate that smaller seed islands are expected to be able to trigger NTMs on ITER [6], and that the β threshold for meta-stability of NTMs will be lower. Coupled with the expectation of strongly fast-particle stabilised sawteeth on ITER, which dramatically lowers thresholds for sawtooth triggered NTMs on JET, a prudent approach is still required for ITER. Thus the continued development of direct 3/2 and 2/1 NTM stabilisation techniques, as well as sawtooth control techniques using current drive near q=1, remains imperative. These results do suggest, however, that if the sawtooth (or other seeding mechanisms) can be suitably controlled and minimised, then NTM onset thresholds on ITER could be substantially higher than presently expected.

ACKNOWLEDGEMENTS

This work was partly funded by the United Kingdom Engineering and Physical Sciences Research Council and by EURATOM, and has been partly conducted under the European Fusion Development Agreement. OS was also partly funded by the Swiss National Science Foundation. RJL was supported by US Department of Energy Contract No. DE-AC03-99ER54463. Thanks are due to Max-Planck Institut für Plasmaphysik and Dr. M. Maraschek for their kind permission to use ASDEX Upgrade data from Ref [1] in Figure 7. Thanks are also due to Dr. D. McDonald for supplying details of JET entries to the ITER H mode database.

REFERENCES

[1]. La Haye, R. J., et al., Phys. Plasmas **7** (2000) 3349.
[2]. Gates, D. A., et al., Nucl. Fus. **37** (1997) 1593.
[3]. La Haye, R. J., et al., Nucl. Fus. **38** (1998) 987.
[4]. Günter, S., et al., Nucl. Fus. **38** (1998) 1431.
[5]. Huysmans, G. T. A., et al., Nucl. Fus. **39** (1999) 1965.
[6]. Sauter, O., et al., Phys. Plasmas **4** (1997) 1654.
[7]. Wilson, H. R., et al., Phys. Plasmas **3,** (1996) 248; Connor, J. W., Waelbroeck, F. L., Wilson, H. R. Phys. Plasmas **8** (2001) 2835.

[8]. Fitzpatrick, R. et al. Phys. Plasmas **2** (1995) 825.
[9]. Poli, E., et al., Phys. Rev. Lett. **88** (2002) 075001.
[10]. Wilson, H. R., et al., Plasma Phys and Control. Fus. **38** (1996) A149.
[11]. Zohm, H. et al., Phys. Plasmas **8** (2001) 2009.
[12]. Sauter, O., et al., Plasma Phys. Control. Fusion **44** (2002) 1999.
[13]. Buttery, R. J. et al., Nucl. Fus. **43** (2003) 69.
[14]. Buttery, R. J. et al., Plasma Phys. Control. Fus. **42** (2000) B61.
[15]. Hegna, C. C., Callen, J. D., and La Haye, R. J. Phys. Plasmas **6** (1999), 130.
[16]. Sauter, O., et al., Phys. Rev. Lett. **88** (2002) 105001.
[17]. Angioni, C. et al., Plasma Phys. Control. Fusion 44 (2002) 205≠222
[18]. Wessterhof, E., et al., Nucl. Fus. **42** (2002) 1324.
[19]. ITER H-mode Database Working Group, Nucl. Fus. **34** (1994) 131.
[20]. Brennan, D., et al., Phys. Plasmas **9** (2002) 2998.
[21]. Brennan, D., et al., to be published in Phys. Plasmas Vol **10** Issue 5 (May 2003).

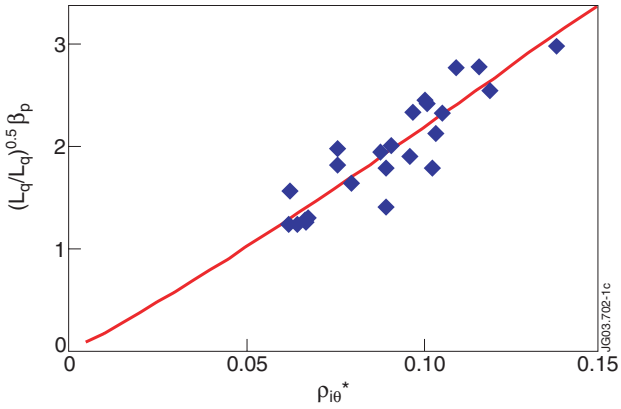

Figure 1: 3/2 NTM onset thresholds in JET, measured in local parameters for q_{95}~3.4 ELMy H-mode NBI-only heated plasmas.

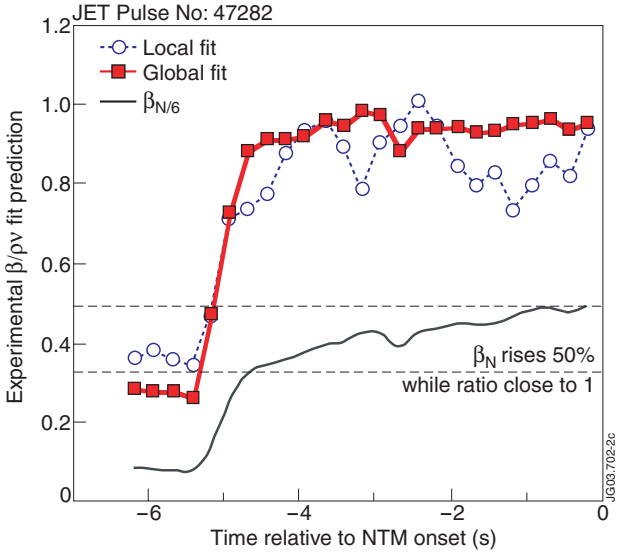

Figure 2: Ratio of experimental β to NTM onset threshold prediction using either a local form, ($[L_q/L_p]\beta_p$ - circles), or global form (β_N - squares), plotted against time prior to NTM onset. Also overlaid (lower trace) is time history of β_N (rescaled).

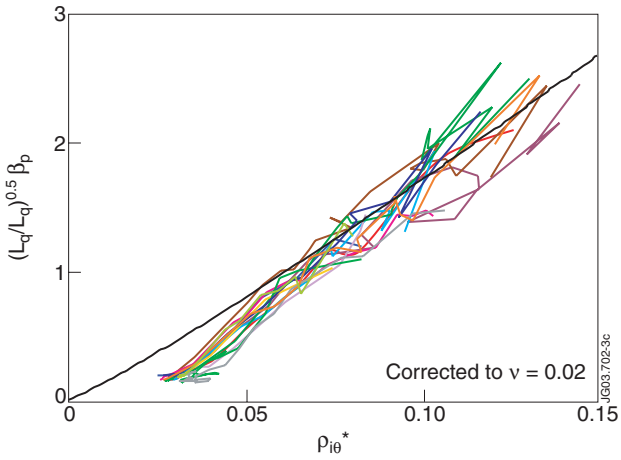

Figure 3: Comparison of local parameter NTM onset scaling with discharge time histories for Pulse No's: 47274-47301 (symbols plotted 0.25s apart) leading up to NTM onset (with NTM onset fit as thick line). Y Ordinate values are corrected for collisionality dependence using Eqn 4.

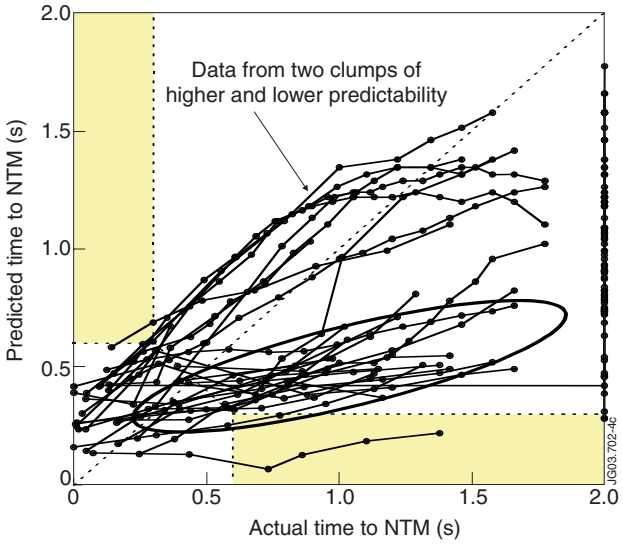

Figure 4: Neural network prediction of time to NTM compared to actual time to NTM for q_{95}~3.4 ELMy H-mode NBI-only heated plasmas using optimum network. Shots which enter the shaded regions are counted as prediction failures ('errors').

Table 1:

Parameters used in network	Value of test residual	Number of errors
β_N $\tau_{sawtooth}$ $\rho_{i\phi}^*$	34.31	6
β_N $\tau_{sawtooth}$	34.41	7
β_N $\rho_{i\phi}^*$	35.68	9
β_N	35.87	11
$\rho_{i\phi}^*$	37.45	10
$\tau_{sawtooth}$	48.85	14
$\tau_{sawtooth}$ $\rho_{i\phi}^*$	37.46	9
β_N ν $\rho_{i\phi}^*$	35.67	10

Table 1: Effect on the test residual and the number of 'errors' (failed predictions) of removing parameters from the optimum neural network (or adding the ν parameter).

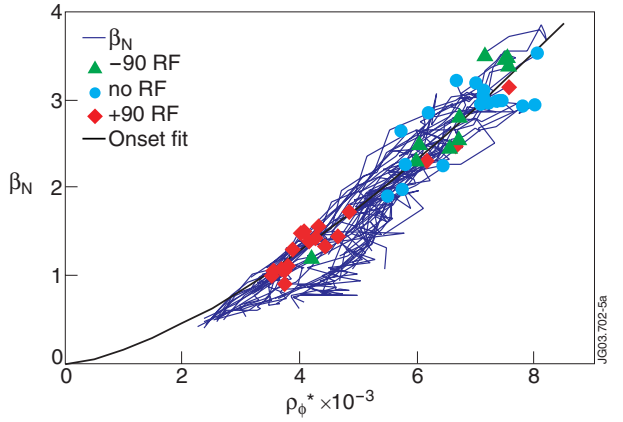

Figure 5(a): Comparison of discharges trajectories (thin lines) and NTM onset points (symbols) on JET where ICRF heating is used to modify sawteeth behaviour (circles: no RF, triangles: -90^o phasing RF; diamonds: $+90^o$ phasing RF). Regression fit to all NTM onset points is also shown, $\beta_N \sim \rho_{i\phi}^{*1.5}$ (thick curve).

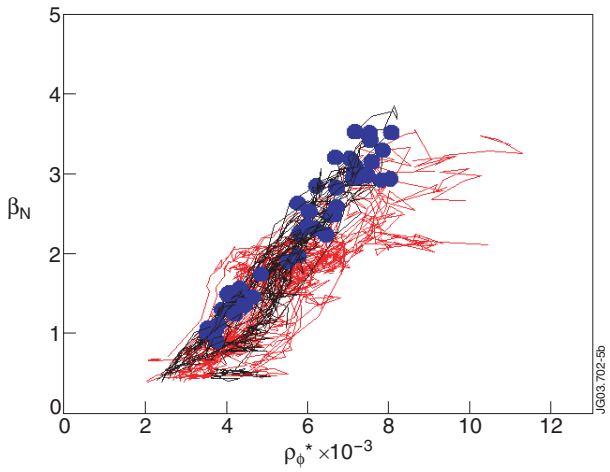

Figure 5(b): Comparison of all NTM onset cases from Fig.5(a) (now all in black with blue circles at NTM onset), with JET data from the ITPA global confinement database (in red) using our definition of $\rho_{i\phi}^*$.

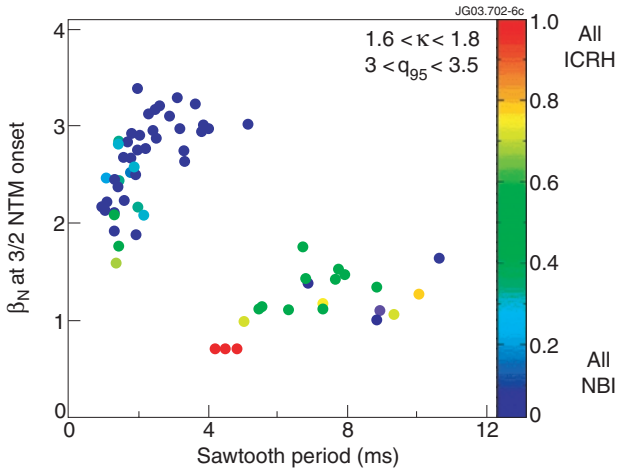

Figure 6: Dependence of NTM onset β_N with sawtooth period for NBI only and core deposition ICRH discharges for standard shape ELMy H modes (right hand colour scale indicates degree of ICRH:NBI power).

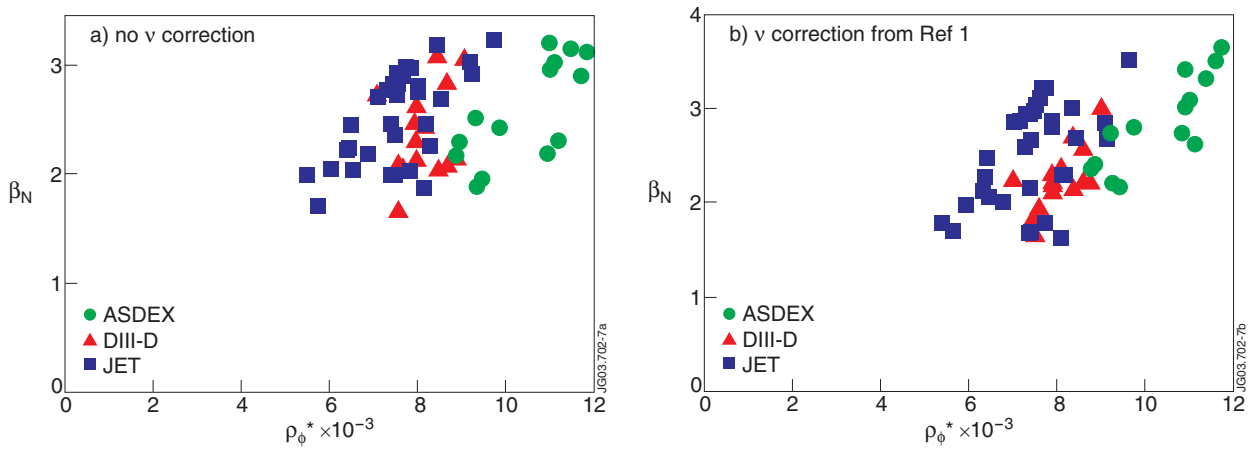

Figure 7: Plot of β_N versus $\rho_{i\phi}^*$ for 3/2 NTM onset cases in similar plasmas from JET (squares), DIII-D (triangles) and ASDEX Upgrade (circles), either as (a) raw data, or (b) corrected for collisionality dependence using best fit from Ref [1]. ITER typical operating point expected at β_N~1.6, $\rho_{i\phi}^*$~0.002.